

Selection of the Optimal Radiotherapy Technique for Locally Advanced Hepatocellular Carcinoma

Ik Jae Lee¹, Jinsil Seong^{1,*}, Woong Sub Koom¹, Yong Bae Kim¹, Byeong Chul Jeon¹, Joo Ho Kim¹ and Kwang Hyub Han²

¹Department of Radiation Oncology and ²Internal Medicine, Yonsei Liver Cancer Clinic, Yonsei University College of Medicine, Seoul, Republic of Korea

*For reprints and all correspondence: Jinsil Seong, Department of Radiation Oncology, Yonsei University Health System, 134 Shinchon-Dong, Seodaemoon-Gu, Seoul 120-752, Republic of Korea. E-mail: jsseong@yuhs.ac

Received October 31, 2010; accepted March 25, 2011

Objective: Various techniques are available for radiotherapy of hepatocellular carcinoma, including three-dimensional conformal radiotherapy, linac-based intensity-modulated radiotherapy and helical tomotherapy. The purpose of this study was to determine the optimal radiotherapy technique for hepatocellular carcinoma.

Methods: Between 2006 and 2007, 12 patients underwent helical tomotherapy for locally advanced hepatocellular carcinoma. Helical tomotherapy computerized radiotherapy planning was compared with the best computerized radiotherapy planning for three-dimensional conformal radiotherapy and linac-based intensity-modulated radiotherapy for the delivery of 60 Gy in 30 fractions. Tumor coverage was assessed by conformity index, radical dose homogeneity index and moderated dose homogeneity index. Computerized radiotherapy planning was also compared according to the tumor location.

Results: Tumor coverage was shown to be significantly superior with helical tomotherapy as assessed by conformity index and moderated dose homogeneity index ($P = 0.002$ and 0.03 , respectively). Helical tomotherapy showed significantly lower irradiated liver volume at 40, 50 and 60 Gy (V40, V50 and V60, $P = 0.04$, 0.03 and 0.01 , respectively). On the contrary, the dose–volume of three-dimensional conformal radiotherapy at V20 was significantly smaller than those of linac-based intensity-modulated radiotherapy and helical tomotherapy in the remaining liver ($P = 0.03$). Linac-based intensity-modulated radiotherapy showed better sparing of the stomach compared with helical tomotherapy in the case of separated lesions in both lobes (12.3 vs. 24.6 Gy). Helical tomotherapy showed the high dose–volume exposure to the left kidney due to helical delivery in the right lobe lesion.

Conclusions: Helical tomotherapy achieved the best tumor coverage of the remaining normal liver. However, helical tomotherapy showed much exposure to the remaining liver at the lower dose region and left kidney.

Key words: hepatocellular carcinoma – 3D-CRT – IMRT – helical tomotherapy

INTRODUCTION

Radiotherapy (RT) of hepatocellular carcinoma (HCC) has long been overlooked for fear that radiation might induce fatal hepatic toxicity at doses lower than therapeutic doses (1,2). However, recent developments in RT technology have overcome this limitation by delivering focused, high-dose, partial liver RT (3–8). In fact, the use of RT in treating HCC is rapidly increasing, as evidenced by the increasing

number of publications in PubMed, from 11 in 1990 to 77 in 2008.

Various RT modes are available from three-dimensional conformal RT (3D-CRT) to more sophisticated techniques including intensity-modulated RT (IMRT) and image-guided RT (IGRT). Of these techniques, 3D-CRT is most commonly used for HCC (9,10). Helical tomotherapy (HT) is a sort of fusion technology that combines IMRT and IGRT

(11,12). Because of its 360° beam arrangement and helical delivery of radiation, HT computerized RT planning (CRTP) may provide equal or better tumor coverage and protection of healthy tissues compared with linac-based step-and-shoot IMRT (L-IMRT) or 3D-CRT CRTP for various tumors (13–15). HT also has wider applications, ranging from total marrow irradiation to radiosurgery (16,17); however, the application of HT in HCC has been very limited (18,19).

The goal of RT for HCC is to maximize therapeutic effects by escalating the radiation dose while simultaneously sparing the adjacent normal organs. The liver is one of the largest organs of the body; its asymmetric shape has been divided by Couinaud (20) into eight independent segments. Tumor location should be taken into account when performing local RT of HCC to minimize radiation complications not only of the liver but also of adjacent organs.

At Yonsei University, HT has been used to treat HCC since 2006. Although HT is known to provide better dose coverage for tumors in general, the effectiveness of HT for liver tumors specifically is not known. Therefore, we evaluated dose conformity of 3D-CRT, L-IMRT and HT in patients with locally advanced HCC. The purpose of this study was to determine the optimal RT for locally advanced HCC.

PATIENTS AND METHODS

Between August 2006 and December 2007, 12 patients underwent HT for locally advanced HCC. The ‘locally advanced hepatocellular carcinoma’ was defined as the disease not amenable to surgical resection or immediate liver transplantation, and the disease should be locally advanced as defined by BCLC (B) intermediate stage or BCLC (C) advanced stage without extrahepatic spread except regional lymph node involvement (21). A total of six patients (50%) were treated with additional therapy before receiving RT including: transcatheter arterial chemoembolization (TACE), transcatheter arterial chemoinfusion or systemic chemotherapy, and local therapy such as radiofrequency ablation and surgery. In these patients, RT was chosen as a salvage modality aim. For locally advanced HCC such as large tumor or portal vein thrombosis, concurrent chemoradiotherapy with intra-arterial chemoinfusion was done as a definitive aim.

Their HT CRTP was compared with the best CRTPs for 3D-CRT and L-IMRT. HT CRTP was performed with Tomotherapy Hi-Art System® (TomoTherapy, USA), L-IMRT CRTP was performed with Corvus® (Nomos, USA) and 3D-CRT CRTP was performed with the Pinnacle planning system (Philips, USA). The L-IMRT and HT planning systems use different dose calculation algorithms; Corvus® uses a finite-size pencil beam algorithm and calculations were based on the work of Nizin (22), whereas HT uses a superposition convolution algorithm (23). We used heterogeneity correction for both L-IMRT and HT CRTP.

For planning computed tomography (CT) scans, patients were positioned supine with their arms above the head. The BodyFIX® vacuum immobilization system (Medical Intelligence Corp., Germany) was used to reduce the planning target volume (PTV) and minimize patient’s respiratory motion. Planning CT was performed with a helical CT simulator (Marconi, Picker PQ 5000, USA) with 5 mm slice thickness. To verify craniocaudal motion, we also checked diaphragm movement by fluoroscopic imaging during the simulation. The clinical target volume was expanded according to the degree of diaphragm movement to create the PTV, which was prescribed as 60 Gy in 30 fractions. Target volume receiving at least 95% of the prescribed dose should reach values of 100%.

To determine which RT mode provides the best conformal coverage (conformity), two parameters—conformity index (CI) and homogeneity index—were analyzed. CI is defined as the ratio of the treated volume (TV) to the PTV (24)

$$CI = \frac{TV}{PTV}$$

Radical dose homogeneity index (rDHI) and moderate DHI (mDHI) were defined as the ratio of D_{\min} (minimum dose within target volume) to D_{\max} (maximum dose within target volume), and the ratio of $D_{95\%}$ (dose to 95% of target volume) to $D_{5\%}$ (dose to 5% of target volume should be used), respectively (25)

$$rDHI = \frac{D_{\min}}{D_{\max}}$$

$$mDHI = \frac{D_{\geq 95\%}}{D_{\geq 5\%}}$$

The mean dose, V20, V30, V40, V50 and V60 were compared for the remaining normal liver and stomach. We selected three patients with the different locations of the liver lesion. CRTPs were also compared according to the tumor location; three different tumor locations were analyzed, which correspond to Couinaud’s liver segment classification as follows: right lobe lesions, lesions in both lobes and left lobe lesions; right lobe lesions at S5–8 and S5–6, right lobe mass at S5–6, separated lesions at S4 and S5–6, and left lobe lesion. For IMRT CRTP, a non-coplanar technique was also allowed.

RESULTS

COVERAGE OF TARGET VOLUME ALONG THE TUMOR CONTOURS

Patient characteristics including stage, tumor location, volume of target tissue and adjacent normal organs (organs at risk) are displayed in Table 1. The patients staged according to the modified UICC staging classification. Three of them showed portal vein thrombosis. The target volume coverage and dosimetric data of 3D-CRT, L-IMRT and HT

Table 1. Patient characteristics

Case no.	Age/sex	Stage	Child–Pugh class	GTV (cc)	Organs at risk			Tumor location
					Remaining liver (cc)	Stomach (cc)	Small bowel (cc)	
1	48/M	T3N0	A	483.4	1760.2	565.9	452.4	S4
2	62/F	T4N1	B	228.2	1110.9	160.5	416.2	Lt. lobe with L/N metastasis
3	64/M	T4N0	A	1280.4	942.7	248.9	972.1	S4, PVT
4	79/M	T4N0	A	396.7	1696.6	206.6	754.9	Rt. lobe and S4 (separated lesions)
5	55/M	T3N0	A	297.9	823.7	141.1	654.9	S4
6	53/M	T4N0	A	307.1	894.9	232.6	451.8	Rt. lobe (S6), PVT
7	55/M	T3N0	A	203.1	1331.8	209.0	884.3	S2 and S5 (separated lesions)
8	59/M	T3N0	A	425.4	1042.3	429.9	150.2	Lt. lobe
9	56/M	T4N0	A	372.2	1165.4	232.7	232.7	Rt. lobe (S5 and 6)
10	48/M	T4N0	A	2079.9	917.0	138.0	856.8	Rt. lobe (S5–8), PVT
11	64/M	T4N0	A	490.7	1775.2	359.5	302.1	Lt. lobe
12	52/M	T3N0	A	177.9	1536.6	141.0	408.1	Rt. lobe (S5)

GTV, gross tumor volume; Lt., left; L/N, lymph node; PVT, portal vein thrombosis; Rt., right.

Table 2. The target volume coverage and dosimetric data of three-dimensional conformal radiotherapy, linac-based intensity-modulated radiotherapy and helical tomotherapy

Case no.	CI			rDHI			mDHI		
	3D-CRT	L-IMRT	HT	3D-CRT	L-IMRT	HT	3D-CRT	L-IMRT	HT
1	2.32	1.05	1.03	0.79	0.80	0.84	0.90	0.91	0.93
2	2.15	1.12	1.04	0.83	0.84	0.87	0.90	0.91	0.94
3	1.65	1.05	1.04	0.45	0.39	0.69	0.91	0.86	0.89
4	1.83	1.24	1.08	0.81	0.82	0.83	0.92	0.90	0.91
5	1.59	1.12	1.04	0.82	0.83	0.85	0.90	0.91	0.94
6	1.72	1.18	1.07	0.82	0.83	0.83	0.94	0.91	0.92
7	5.86	1.12	1.06	0.76	0.82	0.84	0.84	0.90	0.93
8	2.05	1.11	1.04	0.81	0.82	0.84	0.88	0.90	0.93
9	1.61	1.38	1.19	0.67	0.82	0.83	0.93	0.94	0.98
10	2.11	1.99	1.10	0.77	0.81	0.82	0.90	0.93	0.95
11	1.34	1.19	1.11	0.80	0.82	0.83	0.95	0.97	0.98
12	1.41	1.25	1.12	0.77	0.78	0.80	0.89	0.92	0.93
Mean	2.14 ± 1.16	1.23 ± 0.25	1.07 ± 0.05	0.75 ± 0.11	0.78 ± 0.12	0.82 ± 0.05	0.91 ± 0.03	0.91 ± 0.03	0.93 ± 0.02
P value		0.002			0.28			0.03	

CI, conformity index; rDHI, radical dose homogeneity index; mDHI, moderate dose homogeneity index; 3D-CRT, three-dimensional conformal radiotherapy; L-IMRT, linac-based intensity modulated radiotherapy; HT, helical tomotherapy.

CRTP for 12 patients are shown in Table 2. The CI and mDHI were significantly improved with HT CRTP compared with the 3D-CRT and L-IMRT CRTPs ($P = 0.002$ and 0.03 , respectively). rDHI of HT CRTP also improved, but did not show statistically significant difference.

SPARING OF ADJACENT NORMAL ORGANS

The dosimetric data of 3D-CRT, L-IMRT and HT for the remaining normal liver, stomach and small bowel are shown in Table 3. The high-dose region, the volume fraction of the

remaining liver receiving more than 40 Gy (V40) in HT CRTP, was smaller compared with the other RT techniques. For the low-dose region (V20), the volume fraction of the remaining liver of 3D-CRT was significantly smaller than

Table 3. Dosimetric data of 3D-CRT, L-IMRT and HT for the remaining normal liver and stomach

Organs at risk	3D-CRT	L-IMRT	HT	P value
Remaining liver				
Mean dose (Gy)	20.9 ± 6.8	22.6 ± 11.4	24.9 ± 7.6	0.01
V20 (%)	42.04 ± 14.35	71.07 ± 23.44	65.78 ± 22.4	0.03
V30 (%)	30.11 ± 11.09	50.01 ± 18.02	39.61 ± 17.95	0.07
V40 (%)	17.8 ± 10.3	29.4 ± 12.1	17.8 ± 13.8	0.04
V50 (%)	11.1 ± 6.7	15.3 ± 7.5	7.6 ± 6.1	0.03
V60 (%)	3.9 ± 3.2	2.1 ± 1.5	0.4 ± 0.3	0.01
Stomach				
Mean dose (Gy)	16.1 ± 10.4	22.6 ± 5.7	21.3 ± 6.3	0.11
V40 (%)	10.1 ± 17.3	7.5 ± 11.3	4.6 ± 11.0	0.62
V50 (%)	6.8 ± 13.4	2.6 ± 6.1	2.0 ± 6.0	0.39
V60 (%)	2.7 ± 6.0	0.4 ± 1.1	0.5 ± 1.6	0.24
Small bowel				
Mean dose (Gy)	10.14 ± 6.9	14.74 ± 5.67	14.38 ± 4.71	0.12
V40 (%)	6.49 ± 8.83	5.4 ± 8.33	4.59 ± 1.32	0.67
V50 (%)	3.39 ± 4.59	2.53 ± 3.83	1.54 ± 1.66	0.46
V60 (%)	0.47 ± 0.81	0.22 ± 0.59	0.06 ± 0.17	0.23

those of L-IMRT and HT ($P = 0.03$). Table 3 shows a significant reduction in irradiated fractional volume of the remaining normal liver at V40 ($P = 0.04$), V50 ($P = 0.03$) and V60 ($P = 0.01$) by HT CRTP. HT CRTP also reduced the volume fraction of the stomach receiving more than 40 Gy (54.5 and 38.3% compared with 3D-CRT and L-IMRT, respectively); however, this reduction was not significant (Table 3). The V50 and V60 of the stomach were also decreased with HT CRTP, but this was not significant. The volume of high-dose area (V40, V50 and V60) of the small bowel was also decreased with HT CRTP, but this was not significant. The mean doses for the stomach, small bowel and remaining normal liver using L-IMRT and HT CRTP were higher than the mean doses using 3D-CRT CRTP.

Radiation dosimetric displays for 3D-CRT, L-IMRT and HT CRTP are shown in Fig. 1 according to the tumor location. The V50 of the remaining normal liver was decreased by L-IMRT and HT CRTP for the right lobe lesion; however, 3D-CRT CRTP achieved better sparing of the adjacent organs in the low-dose region (Fig. 2). The mean doses for the remaining normal liver with 3D-CRT and L-IMRT (14.2 and 15.7 Gy, respectively) were lower compared with HT (19.3 Gy). For separated lesions in both lobes, the mean doses for the remaining normal liver were not significantly different among the RT techniques (25.8–27.63 Gy). For the left lobe lesion, 3D-CRT and L-IMRT CRTP achieved lower mean doses for the remaining normal liver (14.9 and 15.9 Gy, respectively) compared with HT (22.3 Gy). However, a dose reduction in the stomach V50 (3.4%) was observed with HT CRTP compared with

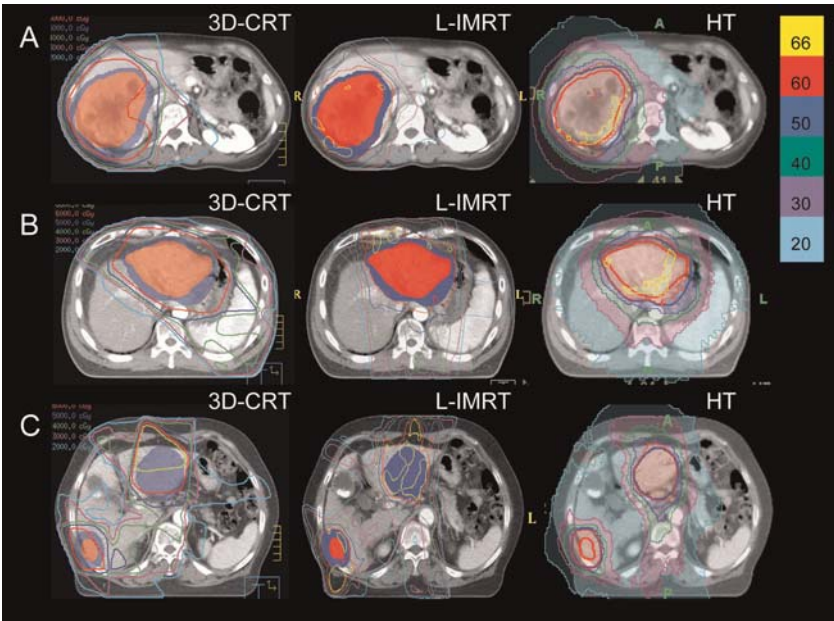


Figure 1. Axial isodose distributions of three-dimensional conformal RT (3D-CRT), linac-based intensity-modulated RT (L-IMRT) and helical tomotherapy (HT). (A) Isodose distributions of 3D-CRT, L-IMRT and HT for the right lobe lesion. (B) Isodose distributions of 3D-CRT, L-IMRT and HT for the left lobe lesion. (C) Isodose distributions of 3D-CRT, L-IMRT and HT for separated lesions at both. Color coding for the isodose color washes ranges from 20 Gy color washes (light blue) to 66 Gy color washes (yellow).

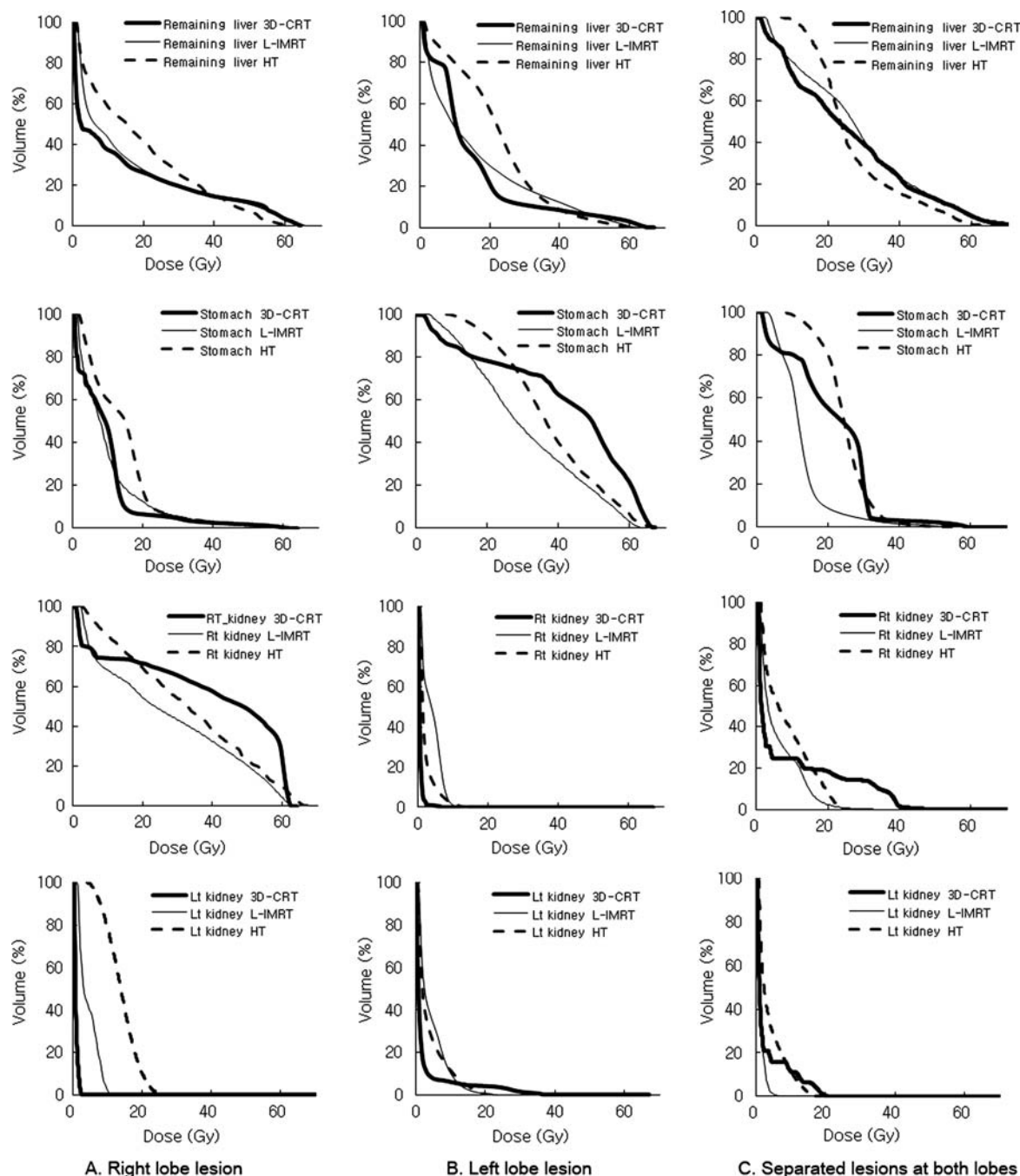


Figure 2. Dose–volume histograms of the remaining liver, stomach, right kidney and left kidney according to the tumor location; (A) right lobe lesion, (B) left lobe lesion and (C) separated lesions at both lobes.

3D-CRT and L-IMRT (5.9 and 5.8%, respectively) in the high-dose region.

Dose–volume histograms (DVH) of the stomach are displayed for 3D-CRT, L-IMRT and HT in Fig. 2. For the separated lesion in both lobes, the mean stomach doses for 3D-CRT, L-IMRT and HT were 20.9, 12.3 and 24.6 Gy, respectively. For the left lobe lesion, the mean stomach doses for 3D-CRT, L-IMRT and HT were 41.6, 30.6 and 37.6 Gy, respectively. The V50 values for 3D-CRT, L-IMRT and HT were 48.1, 16.9 and 21.0%, respectively. A

conformal treatment plan for L-IMRT was successfully generated with decreased mean stomach dose in cases of the separated lesion in both lobes and left lobe lesion (12.3 and 30.6 Gy, respectively). The DVH of the right kidney and left kidney are also displayed in Fig. 2. In the right lobe lesion and separated lesions at both lobes, L-IMRT resulted in less exposed to the right kidney and left kidney than 3D-CRT and tomotherapy, respectively. HT plan showed the high dose–volume exposure to the left kidney due to helical delivery in the right lobe lesion.

DISCUSSION

For patients with locally advanced HCC, several factors should be considered while selecting appropriate RT technique. Although 3D-CRT has been the most commonly used technique for HCC (9,10), analysis of dosimetric plans for 3D-CRT, L-IMRT and HT is needed to compare target coverage and organ sparing. HT delivers its dose from 360° and may produce detrimental effects on non-tumor liver tissue. Cheng et al. (26) compared dose–volume data between 3D-CRT and L-IMRT for patients with HCC. They found that L-IMRT achieved a large dose reduction in the spinal cord and spared the kidney and stomach. L-IMRT exerted diverse dosimetric effects on the liver, significantly reducing the normal tissue complication probability ($P = 0.009$), but significantly increasing the mean dose compared with 3D-CRT ($P = 0.009$). Some studies have reported improved sparing of adjacent normal organs when using HT in various tumors, and HT offers increased dose conformity to the tumor and reduces doses received by sensitive structures (13,14). In the present study, we found that HT decreased high-dose radiation to certain critical structures like the stomach, whereas the mean hepatic dose was increased.

Proton therapy is a type of positively charged particle therapy with a unique dose distribution which makes them suitable for the treatment of deep tumors surrounded by normal structures. Several authors reviewed clinical outcomes of the HCC patients treated with proton beam therapy (PBT) (27–29). Recently, Kawashima et al. (30) reported Phase II study proton therapy for HCC. Thirty patients were enrolled between May 1999 and February 2003. After a median follow-up period of 31 months (16–54 months), only one patient experienced recurrence of the primary tumor, and the 2-year actuarial local progression-free rate was 96%. The actuarial overall survival rate at 2 years was 66% (48–84%). Li et al. (31) conducted a comparative dose distribution study of treatment planning between PBT, 3D-CRT and IMRT in the treatment of HCC, so as to assess the potential advantages of PBT. DVH were compared between PBT and 3D-CRT or IMRT planning at a total dose of 66 and 86 Gy in Stage I patients ($n = 10$, diameter ≤ 5 cm), 60 and 72 Gy in Stage IIA patients ($n = 12$, diameter = 5.1–10 cm). Compared with 3D-CRT and IMRT, PBT significantly reduced the D_{mean} , V10, V20 and V30 in all patients. PBT reduced the dose to the right kidney and stomach significantly. No significant difference was observed respect to the dose to spinal cord. Further study of dose distribution in the treatment of advanced HCC might be necessary, because this study compared only Stage I and IIA disease.

The liver is one of the largest organs of the body; its triangular shape renders different adjacent organs such as the duodenum, colon, small bowels and kidney vulnerable depending on the liver segment involved (20). Park et al. reported that the incidence of acute morbidity was significantly affected depending on the lobe that was irradiated.

Among the 47 patients who underwent 3D-CRT on the right lobe only, 26 patients (55.3%) developed acute morbidity, including nausea and vomiting. In contrast, 11 of 12 patients (91.7%) irradiated on the left lobe developed acute morbidity (8). In our previous study of HCC patients who were treated with 3D-CRT combined with transarterial chemoembolization (TACE), seven patients (14%) developed a gastroduodenal side effect, six patients (12%) developed radiation-induced liver disease and one patient (2%) developed subacute colitis after irradiation of a tumor in segment 5 of the liver (9).

Depending on the tumor location, non-coplanar L-IMRT may improve stomach sparing in patients with left lobe lesions and separated lesions in both lobes. However, non-coplanar L-IMRT generally takes more time because automatic field sequencing is not possible and extra time is required for couch moving. In addition, HT effects may vary depending on the tumor location. Patients with a large centrally located tumor may have more normal liver tissue surrounding the target, which inevitably results in more liver volume receiving radiation and an increased mean hepatic dose. With delivery by HT, improved dose conformity to the tumor targets is achieved with the price of increased mean hepatic dose.

In the case of HCC patients with left lobe lesions, we can protect the right lobe with a directional beam blocking technique as shown in Fig. 3. Directional blocking allows a beam to pass through a given structure only after passing through the PTV, such that the structure receives the exit dose but not the entrance dose (32). HT CRTP with directional beam blocking for the right lobe produced a mean dose for the remaining liver (16.2 Gy) that was similar to that produced by 3D-CRT and L-IMRT (14.9 and 15.9 Gy, respectively) and improved the remaining liver dose compared with conventional HT (22.3 Gy).

Finally, the liver moves with respiration, so tumor movement due to respiration should be considered when applying RT. A limitation of the present study is the interplay effect between the multileaf collimator and tumor motion in HT. A recent study using motion phantoms measured the interplay of parameters between HT deliver and target motion and concluded that HT delivery was not affected by tumor motion (33). In our previous study, the interfractional shift pattern was assessed according to the tumor location (34). We suggested that a more sophisticated approach is required in the free-breathing mode when the left lobe of the liver is irradiated to avoid stomach toxicity. It may also important to reduce motion or gating during HT to reduce the target margins. Therefore, we use the BodyFIX® vacuum immobilization (Medical Intelligence Corp., Germany) to decrease the PTV and minimize patient's respiratory motion.

Because complete necrosis is seldom observed with monotherapy such as 3D-CRT, multimodality therapy may be useful in patients with locally advanced HCC (7,9). We previously reported that concurrent chemoradiation therapy followed by hepatic arterial infusion chemotherapy for advanced HCC with portal vein thrombosis substantially

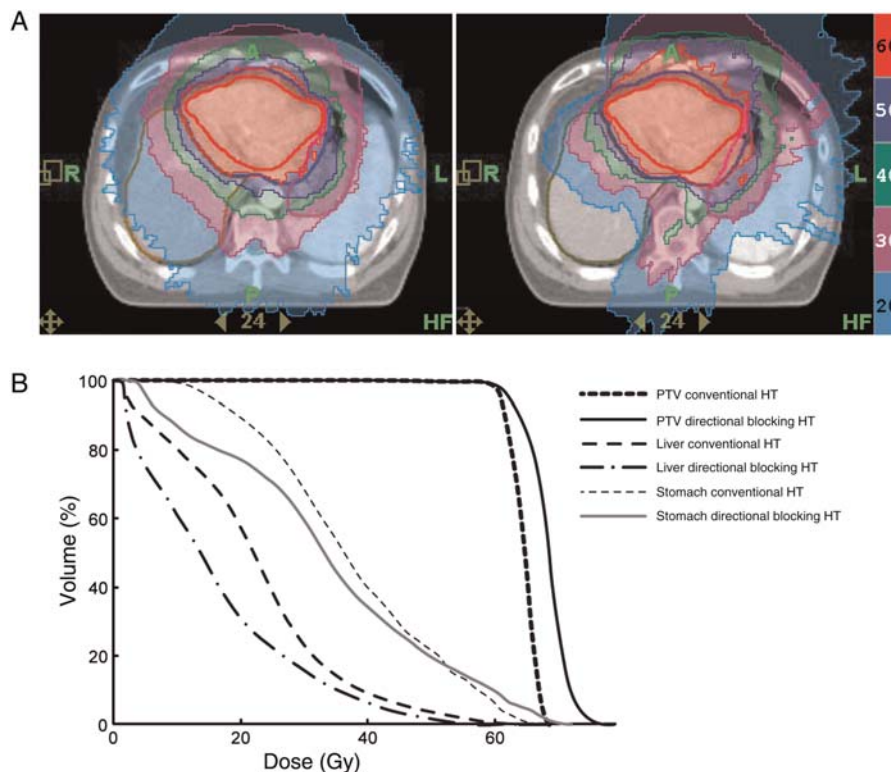


Figure 3. (A) Isodose distribution of conventional HT (left panel) and HT with directional beam blocking of the right lobe (right panel) in a patient with a left lobe lesion. (B) Dose–volume histograms for the planning target volume, remaining normal liver and stomach. HT with directional beam blocking of the right lobe reduced the remaining liver dose compared with conventional HT (16.2 and 22.3 Gy, respectively).

improved the response rate and median survival time (35). McIntosh et al. (18) assessed the initial clinical experience with HT plus capecitabine in patients with large HCC lesions and found acceptable toxicity with promising local control. Therefore, prospective trials are needed to evaluate concurrent chemoradiation therapy with radiation dose escalation by HT for locally advanced HCC.

CONCLUSIONS

Compared with L-IMRT and 3D-CRT, HT provided the best tumor coverage of the remaining liver. However, HT showed much exposure to the remaining liver at the lower dose region and left kidney. For patients with separated lesions in both lobes, L-IMRT offered better sparing of the stomach.

Acknowledgements

This study was presented at the 50th annual meeting of the American Society for Therapeutic Radiation Oncology (ASTRO) in Boston, PA, USA, 21–25 September 2008.

Funding

This work was supported by a faculty research grant of Yonsei University College of Medicine for 2007

(6-2007-0137) and by a National R&D Program grant for cancer control, Ministry of Health and Welfare (0620390).

Conflict of interest statement

None declared.

References

1. Cochrane AM, Murray-Lyon IM, Brinkley DM, Williams R. Quadruple chemotherapy versus radiotherapy in treatment of primary hepatocellular carcinoma. *Cancer* 1977;40:609–14.
2. Ingold JA, Reed GB, Kaplan HS, Bagshaw MA. Radiation hepatitis. *Am J Roentgenol Radium Ther Nucl Med* 1965;93:200–8.
3. Lawrence TS, Tesser RJ, ten Haken RK. An application of dose volume histograms to the treatment of intrahepatic malignancies with radiation therapy. *Int J Radiat Oncol Biol Phys* 1990;19:1041–7.
4. Lawrence TS, Ten Haken RK, Kessler ML, Robertson JM, Lyman JT, Lavigne ML, et al. The use of 3-D dose volume analysis to predict radiation hepatitis. *Int J Radiat Oncol Biol Phys* 1992;23:781–8.
5. Robertson JM, McGinn CJ, Walker S, Marx MV, Kessler ML, Ensminger WD, et al. A phase I trial of hepatic arterial bromodeoxyuridine and conformal radiation therapy for patients with primary hepatobiliary cancers or colorectal liver metastases. *Int J Radiat Oncol Biol Phys* 1997;39:1087–92.
6. Seong J, Keum KC, Han KH, Lee DY, Lee JT, Chon CY, et al. Combined transcatheter arterial chemoembolization and local radiotherapy of unresectable hepatocellular carcinoma. *Int J Radiat Oncol Biol Phys* 1999;43:393–7.
7. Shim SJ, Seong J, Han KH, Chon CY, Suh CO, Lee JT. Local radiotherapy as a complement to incomplete transcatheter arterial

- chemoembolization in locally advanced hepatocellular carcinoma. *Liver Int* 2005;25:1189–96.
8. Park W, Lim do H, Paik SW, Koh KC, Choi MS, Park CK, et al. Local radiotherapy for patients with unresectable hepatocellular carcinoma. *Int J Radiat Oncol Biol Phys* 2005;61:1143–50.
 9. Seong J, Park HC, Han KH, Chon CY, Chu SS, Kim GE, et al. Clinical results of 3-dimensional conformal radiotherapy combined with transarterial chemoembolization for hepatocellular carcinoma in the cirrhotic patients. *Hepatol Res* 2003;27:30–5.
 10. Cheng SH, Lin YM, Chuang VP, Yang PS, Cheng JC, Huang AT, et al. A pilot study of three-dimensional conformal radiotherapy in unresectable hepatocellular carcinoma. *J Gastroenterol Hepatol* 1999;14:1025–33.
 11. Mackie TR, Holmes T, Swerdloff S, Reckwerdt P, Deasy JO, Yang J, et al. Tomotherapy: a new concept for the delivery of dynamic conformal radiotherapy. *Med Phys* 1993;20:1709–19.
 12. Mackie TR, Balog J, Ruchala K, Shepard D, Aldridge S, Fitchard E, et al. Tomotherapy. *Semin Radiat Oncol* 1999;9:108–17.
 13. Cattaneo GM, Dell'oca I, Broggi S, Fiorino C, Perna L, Pasetti M, et al. Treatment planning comparison between conformal radiotherapy and helical tomotherapy in the case of locally advanced-stage NSCLC. *Radiother Oncol* 2008;88:310–8.
 14. Widesott L, Pierelli A, Fiorino C, Dell'oca I, Broggi S, Cattaneo GM, et al. Intensity-modulated proton therapy versus helical tomotherapy in nasopharynx cancer: planning comparison and NTCP evaluation. *Int J Radiat Oncol Biol Phys* 2008;72:589–96.
 15. Kim S, Lee IJ, Kim YB, Koom WS, Jeon BC, Lee CG, et al. A comparison of treatment plans using linac-based intensity-modulated radiation therapy and helical tomotherapy for maxillary sinus carcinoma. *Technol Cancer Res Treat* 2009;8:257–63.
 16. Wong JY, Liu A, Schultheiss T, Popplewell L, Stein A, Rosenthal J, et al. Targeted total marrow irradiation using three-dimensional image-guided tomographic intensity-modulated radiation therapy: an alternative to standard total body irradiation. *Biol Blood Marrow Transplant* 2006;12:306–15.
 17. Penagaricano JA, Yan Y, Shi C, Linskey ME, Ratanatharathorn V. Dosimetric comparison of helical tomotherapy and Gamma Knife stereotactic radiosurgery for single brain metastasis. *Radiat Oncol* 2006;1:26.
 18. McIntosh A, Hagspiel KD, Al-Osaimi AM, Northup P, Caldwell S, Berg C, et al. Accelerated treatment using intensity-modulated radiation therapy plus concurrent capecitabine for unresectable hepatocellular carcinoma. *Cancer* 2009;115:5117–25.
 19. Jang JW, Kay CS, You CR, Kim CW, Bae SH, Choi JY, et al. Simultaneous multitarget irradiation using helical tomotherapy for advanced hepatocellular carcinoma with multiple extrahepatic metastases. *Int J Radiat Oncol Biol Phys* 2009;74:412–8.
 20. Couinaud C. Definition of hepatic anatomical regions and their value during hepatectomy (author's transl). *Chirurgie* 1980;106:103–8.
 21. Llovet JM, Bru C, Bruix J. Prognosis of hepatocellular carcinoma: the BCLC staging classification. *Semin Liver Dis* 1999;19:329–38.
 22. Nizim PS. Electronic equilibrium and primary dose in collimated photon beams. *Med Phys* 1993;20:1721–9.
 23. Mackie TR, Scrimger JW, Battista JJ. A convolution method of calculating dose for 15-MV x rays. *Med Phys* 1985;12:188–96.
 24. International Commission on Radiation Units and Measurements. *ICRU Report 62: Prescribing, Recording and Reporting Photon Beam Therapy*. Bethesda, MD: ICRU, 1999.
 25. Oliver M, Chen J, Wong E, Van Dyk J, Perera F. A treatment planning study comparing whole breast radiation therapy against conformal, IMRT and tomotherapy for accelerated partial breast irradiation. *Radiother Oncol* 2007;82:317–23.
 26. Cheng JC, Wu JK, Huang CM, Liu HS, Huang DY, Tsai SY, et al. Dosimetric analysis and comparison of three-dimensional conformal radiotherapy and intensity-modulated radiation therapy for patients with hepatocellular carcinoma and radiation-induced liver disease. *Int J Radiat Oncol Biol Phys* 2003;56:229–34.
 27. Chiba T, Tokuyue K, Matsuzaki Y, Sugahara S, Chuganji Y, Kagei K, et al. Proton beam therapy for hepatocellular carcinoma: a retrospective review of 162 patients. *Clin Cancer Res* 2005;11:3799–805.
 28. Hata M, Tokuyue K, Sugahara S, Fukumitsu N, Hashimoto T, Ohnishi K, et al. Proton beam therapy for hepatocellular carcinoma with limited treatment options. *Cancer* 2006;107:591–8.
 29. Nakayama H, Sugahara S, Tokita M, Fukuda K, Mizumoto M, Abei M, et al. Proton beam therapy for hepatocellular carcinoma: the University of Tsukuba experience. *Cancer* 2009;115:5499–506.
 30. Kawashima M, Furuse J, Nishio T, Konishi M, Ishii H, Kinoshita T, et al. Phase II study of radiotherapy employing proton beam for hepatocellular carcinoma. *J Clin Oncol* 2005;23:1839–46.
 31. Li JM, Yu JM, Liu SW, Chen Q, Mu XK, Jiang QA, et al. Dose distributions of proton beam therapy for hepatocellular carcinoma: a comparative study of treatment planning with 3D-conformal radiation therapy or intensity-modulated radiation therapy. *Zhonghua Yi Xue Za Zhi* 2009;89:3201–6.
 32. Patel RR, Becker SJ, Das RK, Mackie TR. A dosimetric comparison of accelerated partial breast irradiation techniques: multicatheter interstitial brachytherapy, three-dimensional conformal radiotherapy, and supine versus prone helical tomotherapy. *Int J Radiat Oncol Biol Phys* 2007;68:935–42.
 33. Kanagaki B, Read PW, Molloy JA, Larner JM, Sheng K. A motion phantom study on helical tomotherapy: the dosimetric impacts of delivery technique and motion. *Phys Med Biol* 2007;52:243–55.
 34. You SH, Seong J, Lee IJ, Koom WS, Jeon BC. Treatment margin assessment using mega-voltage computed tomography of a tomotherapy unit in the radiotherapy of a liver tumor. *J Korean Soc Ther Radiol Oncol* 2008;26:280–8.
 35. Han KH, Seong J, Kim JK, Ahn SH, Lee do Y, Chon CY. Pilot clinical trial of localized concurrent chemoradiation therapy for locally advanced hepatocellular carcinoma with portal vein thrombosis. *Cancer* 2008;113:995–1003.